FINAL TECHNICAL REPORT

SPACE GEODETIC CONSTRAINTS ON FAULT SLIP RATES AND THE DISTRIBUTION OF ASEISMIC SLIP ON BAY AREA FAULTS

National Earthquake Hazard Reduction Program

U.S. Geological Survey

NEHRP Program Element: I, Products for Earthquake Loss Reduction

Award Number: 07-HQGR-0109

Principal investigator:

Roland Bürgmann

University of California, Berkeley
Department of Earth and Planetary Science
307 McCone Hall
Berkeley, CA 94720-4767
Telephone: (510) 643-9545;
Fax:(510) 643-9980;
e-mail: burgmann@seismo.berkeley.edu

SPACE GEODETIC CONSTRAINTS ON FAULT SLIP RATES AND THE DISTRIBUTION OF ASEISMIC SLIP ON BAY AREA FAULTS

Award Number: 07-HQGR-0109

Roland Bürgmann

University of California, Berkeley
Department of Earth and Planetary Science
307 McCone Hall
Berkeley, CA 94720-4767
Telephone: (510) 643-9545;
Fax:(510) 643-9980;
E-mail: burgmann@seismo.berkeley.edu

Technical abstract:

This investigation aimed to constrain rates of interseismic strain accumulation and the mechanical properties of crustal fault zones and the lithospher in the San Francisco Bay Area. Measurements of horizontal site velocities using the Global Positioning System (GPS) and range change rates determined with satellite radar interferometry (InSAR) allow us to resolve tectonic surface motions in the region at great precision. The space geodetic measurements provide information on the nature of elastic strain accumulation about seismogenic faults, their locking depth and slip rates, and any variations of those parameters in space and time. In the epicentral region of the M_w = 6.9 1989 Loma Prieta earthquake we see a pattern of converging horizontal motions and subsidence that is found to be consistent with viscous relaxation at depth, primarily in the upper mantle. Densely spaced measurements of deformation about the San Andreas fault in the northern San Francisco Bay area reveal lateral changes of elastic crustal properties across and within the fault zone, consistent with contrasting rock types on either side of the fault and a ~2km-wide fractured and more compliant fault zone.

Non-technical abstract:

Measurements of horizontal site velocities using the Global Positioning System (GPS) and range change rates determined with satellite radar interferometry (InSAR) allow us to resolve tectonic surface motions in the San Francisco Bay Area at great precision. The space geodetic measurements provide information about the rate at which faults slip and about the role of different rock types in the active deformation process. In the region of the 1989 Loma Prieta earthquake we see a pattern of converging horizontal motions and subsidence that is found to be consistent with flow of hot material in the Earth's mantle at depth. Densely spaced measurements of deformation about the San Andreas fault in the northern San Francisco Bay area reveal lateral changes of elastic crustal properties across and within the fault zone, consistent with contrasting rock types on either side of the fault and a ~2km-wide weak fault zone.

SPACE GEODETIC CONSTRAINTS ON FAULT SLIP RATES AND THE DISTRIBUTION OF ASEISMIC SLIP ON BAY AREA FAULTS

1. INTRODUCTION

Imaging strain accumulation about faults with sufficient precision and spatio-temporal resolution is a difficult task, plagued especially by limits in the accuracy and spatial density of the surface measurements. This project incorporates acquisition, processing, analysis and integration of a comprehensive GPS data set for central California, the BAVU time series and velocity field. BAVU is the primary source of central-California data used in ongoing compilations of California-wide velocity fields. The sparsely distributed, but continuously operating CGPS BARD and PBO networks provide a precise geodetic backbone with high temporal resolution into which we integrate campaign-mode measurements collected by our and other groups. Repeated campaign GPS measurements by our group and the USGS provide appropriate densification of precise regional surface deformation to determine long-term strain accumulation rates. The observational program of this project entails GPS measurements of a select subset of stations in our GPS campaign network and processing, archiving and full integration of the campaign GPS data with CGPS data products to produce the repeatedly updated BAVU time series and velocity field. The GPS results together with an increasingly comprehensive and precise InSAR range-change-rate field form the data constraints for models of the deformation and loading of the Bay Area fault system. All data and processed data products are freely available to other researchers.

The data products resulting from the proposed work serve to provide improved constraints for kinematic and dynamic models of regional earthquake-cycle deformation in the Bay Area by our and other research groups. The BAVU data form a major component of the California crustal motion model (SCEC - CMM 4) that is widely used for hazard estimation and defor-mation modeling efforts. Crustal deformation models allow us to translate surface deformation data into information relevant for earthquake hazard. Rigorous kinematic inversions for fault slip rates in the context of a regional rigid block model allow us to interpret the regional deformation pattern and provide geodetic estimates of slip rates on major faults that can be integrated with complementary geophysical and geologic constraints. We evaluate deformation near the San Andreas fault near Pt. Reyes to reveal contrasting elastic properties on either side and weak materials within the fault zone. To properly address time dependent deformation and loading, we developed models that incorporate vertical stratification of both elastic and viscous rheology of

the lithosphere and explore the contributions from postseismic relaxation following the 1989 Loma Prieta. Careful and rigorous consideration of such end-member representations of crustal deformation (rigid elastic blocks vs. deformation dominated by viscous processes at depth) will provide new insights into the deep workings of the Bay Area fault system.

Geodetic measurements provide information on the nature of elastic strain accumulation about seismogenic faults, their locking depth and slip rates, and any variations of those parameters in space and time. This research relies on the analysis and modeling of space geodetic data and interpretation of those results in the context of their mechanical behavior and earthquake potential. GPS and InSAR are complementary techniques for making precise measurements of displacements of the Earth's surface. These can be related to sources of deformation at depth (e.g. faults) by mechanical models. We formally invert the geodetic data for model fault parameters such as depth of locking and slip rate. A report on a complementary investigation relying on PS-INSAR data to illuminate the distribution of aseismic slip and earthquake potential on the Calaveras, Hayward and Rodgers Creek fault system is provide in the Final Technical Report of project 07-HQGR-0077 "Earthquake Potential In The San Francisco Area From PS-InSAR Measurements".

2. CRUSTAL DEFORMATION OBSERVATIONS

2.1 GPS data

Imaging strain accumulation about faults with sufficient precision and spatio-temporal resolution is a difficult task, plagued especially by limits in the accuracy and spatial density of the surface measurements. A mix of campaign mode (SGPS) yearly GPS measurements and data from a core network of continuously operating GPS stations (CGPS) of the BARD and PBO networks contribute to a precise (at mm/yr level) representation of the surface velocity field.Over 10 years of GPS data have now been collected in the San Francisco Bay Area, providing high precision measurements of horizontal surface velocities across the whole plate boundary zone. In this project, we develop and use velocities from the BAVU (Bay Area Velocity Unification) compilation of continuous GPS data from the BARD network and campaign data collected by UC Berkeley and the US Geological Survey since 1994. This project incorporates acquisition, processing, analysis and integration of a comprehensive GPS data set for central California, building on the BAVU velocity field (Figure 1). The sparsely distributed, but continuously operating CGPS BARD and PBO networks provide a precise 3D geodetic framework with high temporal resolution. Repeated campaign GPS measurements in the Bay Area by our group and

data obtained by the USGS provide appropriate densification of precise regional surface velocities to determine long-term strain accumulation rates.

Our GPS analysis relies on the GAMIT/GLOBK processing and analysis system developed at the Massachusetts Institute of Technology [Herring, 2005; King and Bock, 2005]. We include five global stations from the International GPS Service (IGS) network and four to six nearby continuous stations (PPT1, BAY1, JPLM, HARV, GOLD, VNDP) in each of our local processing runs. We combine daily ambiguity-fixed, loosely constrained solutions using the Kalman filter approach implemented by GLOBK. We include data processed locally as well as solutions for the full IGS, PBO and BARD networks processed by SOPAC at the Scripps Institution of Oceanography (http://sopac.ucsd.edu/) and the PBO analysis centers. To reduce errors from strong tropospheric gradients in the SGPS data, we will benefit from troposphere delay maps produced at the BSL every 4 hours, based on analysis of the real-time BARD network. Using the Kalman filter, we combine all daily solutions to generate an average solution for each month, giving each observation equal weight. We then estimate the average linear velocity of each station in the network from these monthly files. We fix the final positions and velocities of the IGS stations into the ITRF2000 global reference frame [Altamimi *et al*., 2002]. We then rotate the solution into a stable North America reference frame by solving for the best fitting relative pole of rotation. One benefit of this data analysis approach lies in the increased ease in which the processing can be integrated with data products from the regional BARD and PBO GPS sites and the global IGS network, which significantly improves the reference stability and also the precision of our velocities. We continue to streamline and automate the BAVU processing scripts which cover all the steps from data downloading to production and posting of time series and velocity tables and maps on the BAVU web page http://seismo.berkeley.edu/~burgmann/RESEARCH/BAVU/index.html.

We scale the measurement errors following the method used by the Southern California Earthquake Center's Crustal Motion Map team (SCEC CMM 3.0; Robert W. King, pers. comm., 2003). We add white noise to the formal uncertainties of all stations with a magnitude of 2 mm/yr for the horizontal components and 5 mm/yr for the vertical component. To account for “benchmark wobble" we add Markov process noise to the solutions with a magnitude of 1 mm $yr^{-1/2}$. For the velocity field shown in Figure 1A we establish a local reference frame centered around station LUTZ (a BARD continuous site on the Bay Block, roughly near the network centroid). We subtract LUTZ's velocity from all stations and propagate the correlations in uncertainty to calculate the error ellipses (95 % confidence intervals) shown in Figure 1.

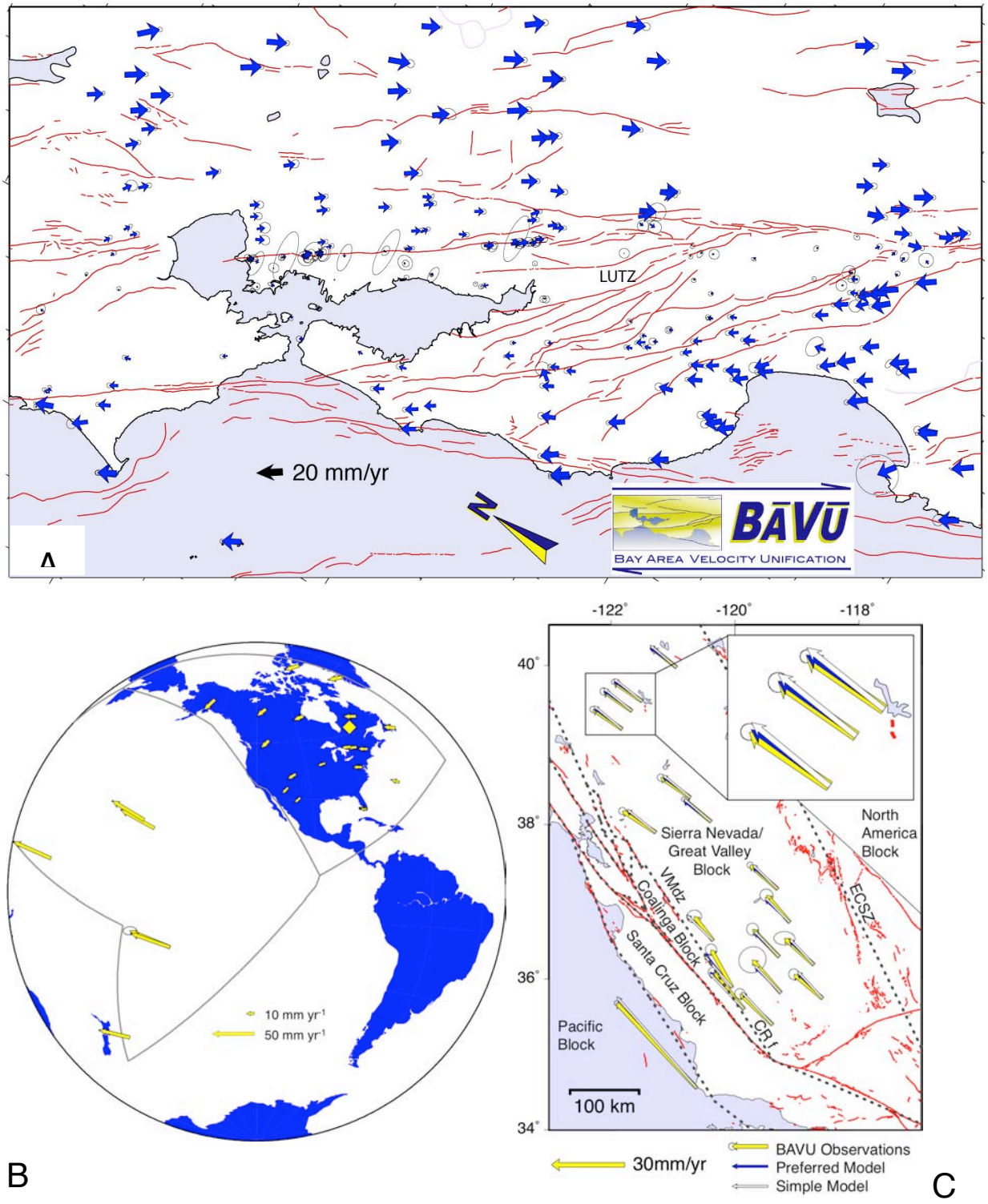

Figure 1. (A) Updated BAVU velocity field referenced to a local site (LUTZ) on the central Bay Block spanning 1994-2006. The map is in an oblique Mercator projection about the pole of Pacific-plate-to-SNGV block rotation. (B) Global and (C) central California scale BAVU velocity field also showing fit of a block model developed by *d'Alessio et al.* (2005).

The BAVU compilation includes survey-mode GPS data from over 200 GPS stations throughout the greater San Francisco Bay Area from Sacramento to San Luis Obispo collected from 1991 to 2007 by U. C. Berkeley, the U.S. Geological Survey, the California Department of Transportation, Stanford University, U. C. Davis and the Geophysical Institute in Fairbanks, AK. These are combined with continuous GPS data from the BARD and PBO networks. BAVU provides a consistent velocity field for monitoring fault slip and strain accumulation throughout the greater San Francisco Bay region.

The BAVU velocity field forms a core component of the recently developed California-wide velocity map, developed by D. Agnew, R. King, Z-K Shen, and M. Murray (Figure 2). This velocity model, recently provided to the California Earthquake Authority (CEA) includes data from the SCEC Crustal Motion Map (CMM 3) (1986-2001), the SCIGN CGPS network (1996-2003), BAVU (1993-2003), and northern California and Pacific Northwest SGPS networks (1993-2004).

We continually update and improve the BAVU time series and velocity solutions for use by the research community, including future version of the crustal motion map . In addition to the role of GPS measurements in allowing for the precise determination of interseismic deformation rates, the existence of a solid geodetic network will also be important as part of the scientific response to the next large earthquake in the Bay Area. Studies of coseismic and postseismic deformation will greatly benefit from a well-developed network of continuously operating CGPS and survey-mode SGPS sites. Such data will be used to develop kinematic models of earthquake ruptures to aid in better understanding of source characteristics. The slowly increasing number of CGPS sites in the region (especially thanks to PBO) and availability of InSAR have allowed us to reduce and focus the SGPS surveys, but do not make them expendable.

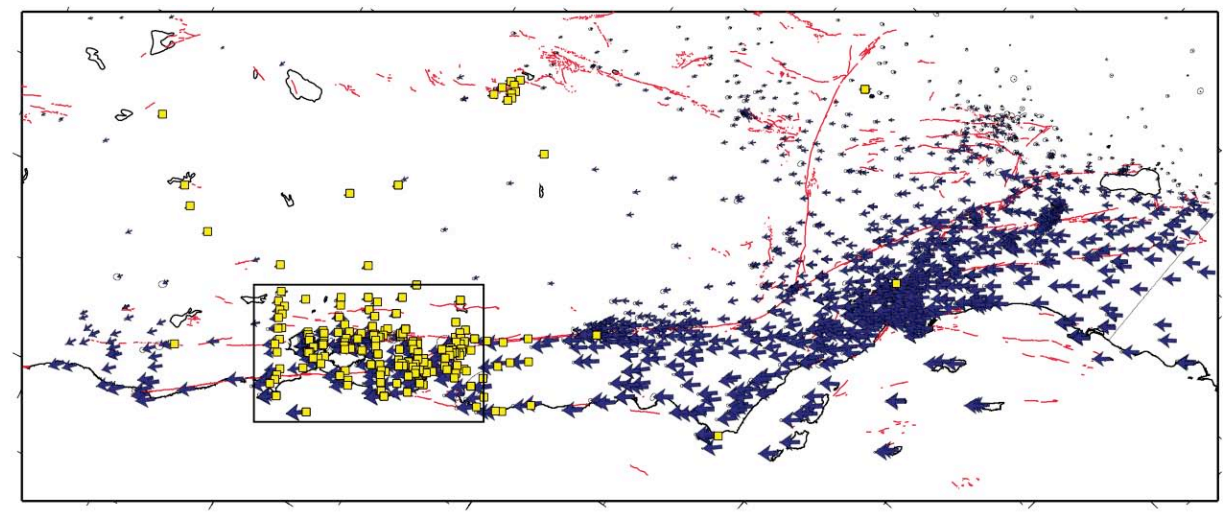

A

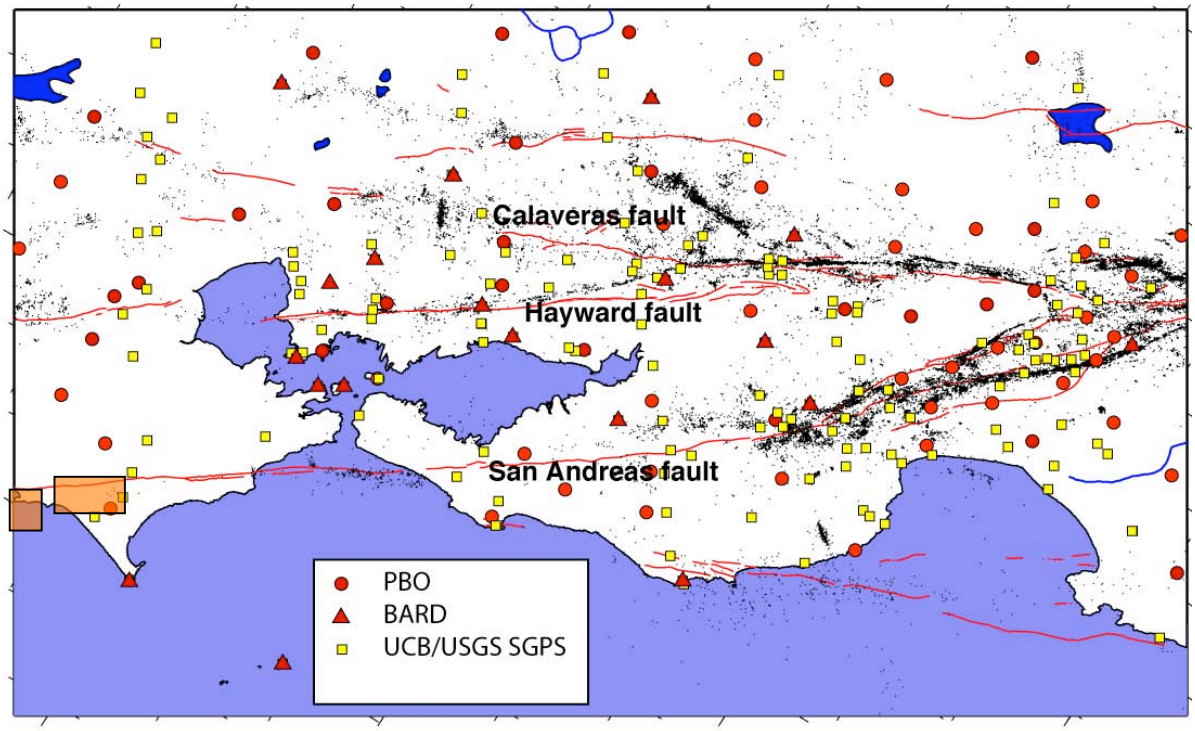

B

Figure 2. (A) BAVU sites shown together with California-wide velocities of the Crustal Motion Map (CMM 4.0) compiled by King, Agnew, Shen and Murray. Boxed area shows close-up in (B). (B) Station map of continuous (circles are PBO triangles are BARD) and campaign GPS networks (USGS and UCB, yellow squares) in the San Francisco Bay Area. Here we present preliminary results from our study of near-fault sites along the San Andreas in the Pt. Reyes region (outlined by transparent boxes), and the epicentral area of the Loma Prieta earthquake. The updated BAVU data set includes latest data from all stations shown, in addition to regional and global CGPS sites and all BAVU raw data and data products are made available to other researchers.

2.2 PS-InSAR data

InSAR provides a one-dimensional measurement of change in distance along the look direction of the radar spacecraft. Given the orientation of the track direction of polar, sun-synchronous satellites, this measurement is affected by deformation in both horizontal components and, particularly, in the vertical. We have had significant success in the recent past in applying conventional InSAR to both the horizontal and the vertical surface deformation in the San Francisco Bay Area, revealing cm-level uplift and subsidence patterns related to the seasonal drawdown and recharge of the Santa Clara valley aquifer [Schmidt and Bürgmann, 2003]; rapid motions of deep-seated landslides [Hilley *et al*., 2004]; a possible sub-mm/yr contribution of an east-side-up, dip-slip component to the range change offset across the creeping northern Hayward fault [Hilley *et al*., 2004; Schmidt *et al*., 2005]; and allowing the estimation of the distribution of fault creep on the Hayward fault, and therefore the extent of the part of that fault that remains locked [Schmidt *et al*., 2005]. Recent work during the project period using the PS-InSAR data in conjunction with our GPS measurements has focused on resolving vertical motion in the Bay region [Bürgmann *et al*., 2006] and on resolving aseismic slip on the Hayward-Rodgers Creek faults [Funning *et al*., 2007].

We incorporate 49 European Remote Sensing satellite (ERS-1 and 2) acquisitions collected from 1992 to 2000 of our Bay Area target scene (track 70, frame 2853) and a 35 image dataset collected by the RADARSAT-1 spacecraft (Figure 3). Points whose displacements vary in a highly non-linear fashion, such as a large area of rapid seasonal uplift and subsidence in the Santa Clara Valley [Schmidt and Bürgmann, 2003] are excluded from the final data set. The PS-InSAR data provide range-change rates at > 100,000 points including targets in vegetated or mountainous areas that are unsuitable for standard InSAR. In addition, these datasets contains a time-series of displacement, which allows us to identify regions in which there is a significant time-varying, often seasonal component to the deformation field.

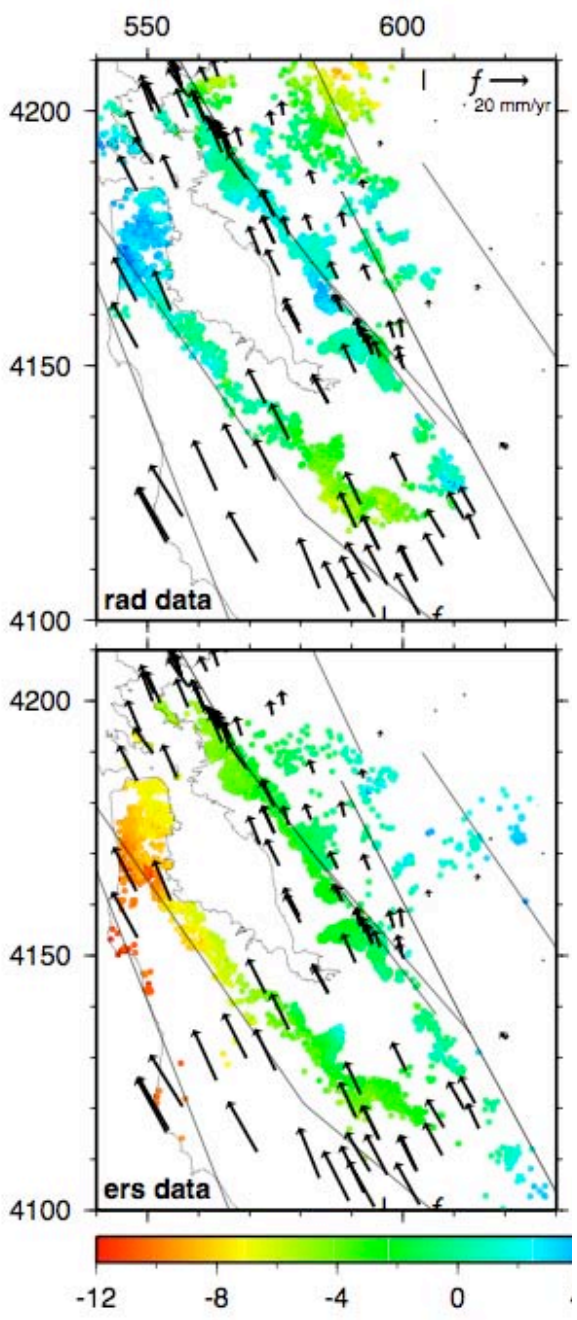

Figure 3. Left: PS-InSAR surface deformation rate data used in this study (rad: RADARSAT-1 data, ers: ERS-1/2 data). Each colored dot on land indicates the location of a permanent scatterer on the ground; red colors indicate points where the distance, or range, between the satellite and the ground increases with successive satellite passes (i.e. movement away from the satellite), blue colors indicate movement towards the satellite.

When interpreted in terms of vertical motions, the residual range-change rate field of bedrock target points includes three larger areas of subsidence and three regions of uplift at 0.5-1.5 mm/yr rate. One area of apparent subsidence is located east of the Greenville fault and we have no obvious explanation for this feature. The second area of subsidence at rates of up to ~2 mm/yr appears localized about the epicentral region of the 1989, $M_w = 6.9$ Loma Prieta earthquake and coincides with the region of horizontal contraction evident in the residual GPS velocities (Figures 3, 4). A third zone of slow (~0.5 mm/yr) subsidence along the northern San Francisco

peninsula may be related to an extensional bend in the SAF and/or interaction with the offshore San Gregorio fault zone. Uplifted regions along the East Bay Hills, the Santa Cruz Mountains to the northeast of the SAF near Black Mountain and in the southern foothills of Mt. Diablo appear to reflect tectonic uplift along restraining discontinuities of Bay Area strike-slip faults [Bürgmann *et al*., 2006].

3. RESULTS

3.1. Post-Loma Prieta earthquake viscous relaxation

An important factor affecting the calculation of earthquake forecasts lies in the details of the initial magnitude and decay rate of the stress shadow of the M_w = 7.8 1906 San Andreas fault earthquake, which apparently relieved stress on neighboring faults sufficiently to produce a rather low number of moderate-to-large earthquakes in the 20th century. Sophisticated models of the Bay Area fault system and the effects of postseismic relaxation from major earthquakes [Kenner and Segall, 2003; Parsons, 2002; Pollitz *et al*., 2005] are primarily constrained and tested by geodetic data. The consideration of time-dependent earthquake hazard, and in particular the role of time-varying earthquake shadows and transiently-stressed zones will allow us to refine earthquake hazard probability estimates. Constraints derived from GPS and PS-InSAR data over the epicentral region of the 1989 Loma Prieta earthquake provide new constraints on the deep rheology of the Bay Area lithosphere.

Figure 4 shows a closeup of the GPS residual velocities after subtracting an interseismic elastic strain accumulation model from the BAVU dataset in the south Bay area near the epicentral region of the 1989 M_w 6.9 Loma Prieta earthquake. Vertical rates are shown for sites for which the formal uncertainty has been determined to be < 2 mm/yr. Also shown are residuals of the PS-InSAR data in the region. We note that the epicentral region appears to undergo right-lateral shear, overall contraction and subsidence during the 1992-2000 time interval.

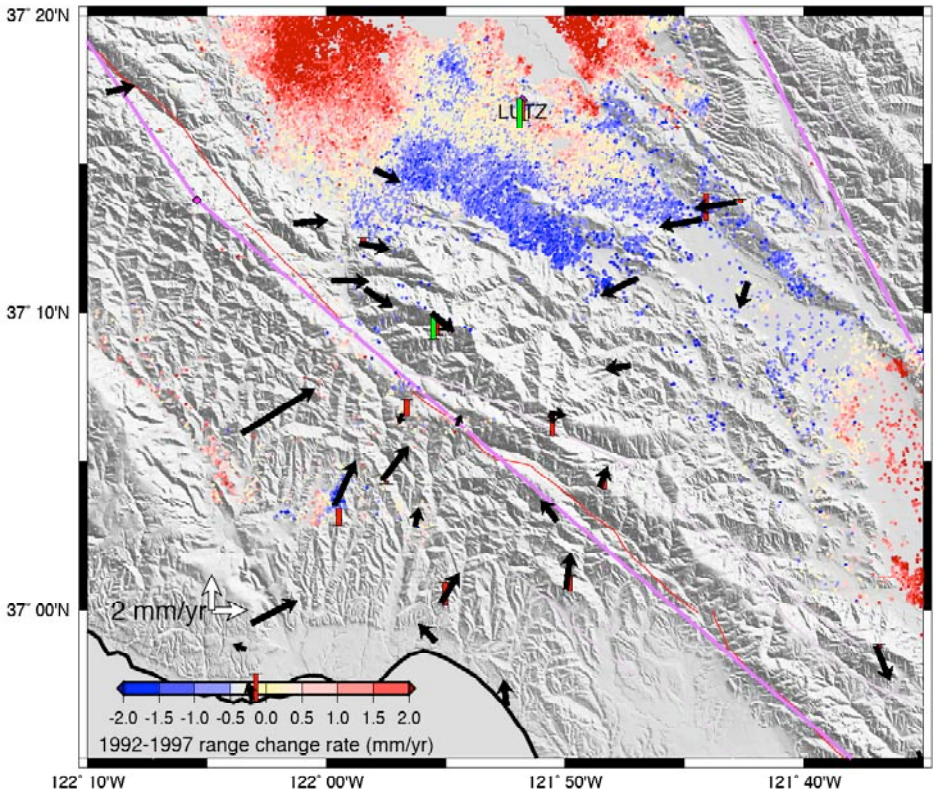

Figure 4. Difference between observed GPS velocities and model calculations in the epicentral region of the Loma Prieta earthquake. Vertical GPS rates are shown for sites with formal V_{up} uncertainties < 2 mm/yr) in the BAVU solution (red bars) and from the SOPAC solution for BARD CGPS sites (green bars).

Of particular interest is distinguishing the deformation resulting from localized afterslip on a narrow aseismic shear zone below a large earthquake rupture from surface strain resulting from distributed viscous flow at depth [*Thatcher*, 1983]. Highly precise measurements of postseismic horizontal and vertical motions can reveal the source mechanics of the transient deformation and allow for determining the appropriate constitutive properties of the relaxing lithosphere.

Deformation measurements during the first 5 years of the postseismic transients following the Loma Prieta earthquake could be attributed to shallow and mid-crustal afterslip. The deformation measured with GPS immediately following the Loma Prieta earthquake revealed significant postseismic contraction and right-lateral shear across the southern Santa Cruz Mountains northeast of the SAF [Bürgmann *et al*., 1997; Savage *et al*., 1994]. The localized nature of the transient displacement field indicates relatively shallow deformation sources. The measurements of the first five years can be interpreted to be due to aseismic right-oblique fault slip on or near the coseismic rupture, as well as thrusting up-dip of the rupture within the Foothills thrust belt [Bürgmann *et al*., 1997]. Analysis of the time-varying nature of the deformation signal suggests that the shallow transient thrusting ceased in 1992 while resolvable oblique shear at seismogenic depths may have persisted through 1994 [Segall *et al*., 2000]. The total moment of the modeled 1989-1994 afterslip on the two sources was ~5 x 10^{18} Nm, about 15 % of the coseismic moment release [Segall *et al*., 2000]. Analysis of the GPS measurements did not resolve a significant

contribution of lower-crustal, or upper-mantle relaxation processes during the first 5 years following the event [Pollitz *et al*., 1998]. Surface displacement measurements using GPS and InSAR help us resolve continued transient strain accumulation in the region, since 1993.

We rely on the residuals of surface deformation measurements from InSAR and GPS measurements following the removal of a modeled interseismic velocity field. We focus on a 200-station, greater Bay Area subset of the regional GPS velocity field to constrain a mechanical model of the horizontal velocity field [Bürgmann *et al*., 2006]. In the model, uniform-slip dislocations in an elastic, homogenous, and isotropic half-space [*Okada*, 1985] reproduce the surface motions about the Bay Area faults, including the contribution of shallow aseismic creep on several faults in the region. A relatively simple 17-element dislocation model can explain much of the observed horizontal velocity field. The Loma Prieta region exhibits a systematic misfit pattern in the residual GPS velocities, where a zone of apparent residual contraction and right-lateral shear of ≤ 5 mm/yr is observed that is not explained by our model. We utilize the residual GPS velocities of 36 sites located within a distance of ≤ ~ 30 km of the epicenter.

We use permanent scatterer InSAR (PS-InSAR) data to add a large number of additional point-displacement measurements and constrain vertical motions in the area [Bürgmann *et al*., 2006]. InSAR provides measurements of change in distance along the look direction of the radar spacecraft and is highly sensitive to vertical motion due to its steep (20-26° off-vertical) look angle [Bürgmann *et al*., 2000]. We use results presented in Bürgmann et al. [2006] relying on 49 European Remote Sensing satellite (ERS-1 and 2) acquisitions of frame 2853 along track 70 collected from 1992 to 2000 (Fig. 1). As motions of points on Quaternary substrate are often impacted by hydrological processes [*Schmidt and Bürgmann*, 2003], we only include points located on pre-Quaternary bedrock units based on the map of Knudsen et al. [2000]. After removing the contribution of background deformation as defined by the GPS-derived dislocation model, residual PS-InSAR rates reveal an area of range increase at rates of up to ~2 mm/yr localized about the epicentral region of the Loma Prieta earthquake, which roughly coincides with the region of horizontal contraction evident in the residual GPS velocities [Bürgmann *et al*., 2006]. The horizontal residual motions indicated by the GPS measurements project to < 0.5 mm/yr of range change; thus, this range-change rate anomaly is dominantly due to subsidence at ~ 2 mm/yr in this region. Here we evaluate if this zone of contraction, right-lateral shear and subsidence is related to late-stage postseismic relaxation from the oblique-reverse earthquake [Pollitz *et al*., 1998].

We consider simple models of postseismic relaxation in a layered visco-elastic representation of the Earth's lithosphere. The model consists of an elastic upper crust (to 15 km depth) underlain by a Maxwell visco-elastic lower crustal layer and visco-elastic mantle half-space. The

calculations are carried out using the VISCO1D program [Pollitz *et al*., 1997] to calculate deformation using spheroidal and toroidal motion modes of the spherically stratified elastic-viscoelastic medium. The model is parameterized by specifying the coseismic fault geometry and slip of the source event and the depth dependent elastic and viscous parameters.

We adopt the coseismic fault model of *Marshall et al*. [1991] to drive the viscous relaxation, but also examine results based on the distributed-slip model by *Arnadottir and Segall* [1994]. The model lithosphere (Figure 5b) consists of an elastic upper crust of thickness 16 km, a Maxwell viscoelastic lower crust of thickness 14 km and viscosity η_c, and a Maxwell viscoelastic upper mantle of viscosity η_m, following a model developed by *Pollitz et al*. [1998]. Figure 5a shows the predicted average horizontal velocities and range-change rates during the observation time period assuming relaxation in a mantle with Maxwell viscosity of 0.86×10^{19} Pa s and a lower crust represented by a standard linear solid with a viscosity of 2.9×10^{18} Pa s. The first-order pattern of predicted deformation from these models matches the InSAR observations well. The modeled horizontal deformation appears to produce much of the observed fault-normal contraction, but does not appear to do a good job in reproducing the amount and distribution of fault parallel motions. This may be due to limitations in our ability to separate and remove "background" interseismic motions from the observed deformation using the deep-slip dislocation model we employ.

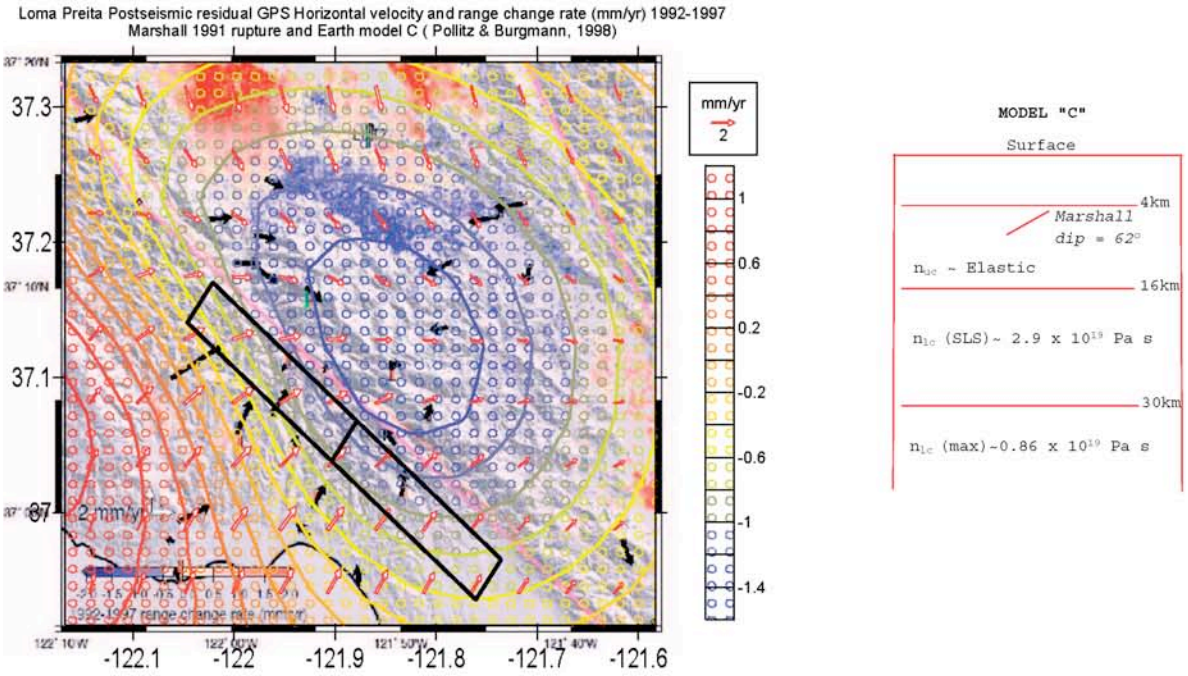

A **B**

Figure 5. (a) Comparison of observed GPS-measured horizontal and InSAR-measured LOS range-change residuals from an interseismic dislocation model with predicted deformation from the layered visco-elastic lithosphere model shown in **(b)** using the coseismic source model of *Marshall et al.* [1991].

We are now exploring a suite of model runs using the *Marshall et al*. [1991] and *Arnadottir and Segall* [1994] source models to comprehensively evaluate the misfit to the data (weighted sum of squared residuals, WRSS) with respect to the elastic plate thickness and mantle viscosity chosen. A manuscript (Bürgmann et al., Viscous Post 1989 Loma Prieta Earthquake Relaxation From 1993 – 2004 GPS and Permanent Scatterer InSAR Data) is in preparation to report on this work.

3.2. GPS exploration of the elastic properties across and within the Northern San Andreas Fault zone

Earthquake cycle deformation is commonly modeled assuming laterally homogeneous elastic properties in the Earth's crust. Interseismic deformation models are often based on an elastic half-space, sliced by an infinitely deep and infinitely long dislocation below seismogenic depth [Savage and Burford, 1973]. First-order variations in rock elastic strength both across and within fault zones can impact inferences of fault slip parameters and earthquake rupture characteristics in a homogeneous model [Chen and Freymueller, 2002; Jolivet *et al*., 2008b; Le Pichon *et al*., 2005; Schmalzle *et al*., 2006]. Here we focus on the effects of such lateral rheological variations

across and within the San Andreas fault (SAF) zone on the interpretation of space geodetically measured surface deformation [Jolivet *et al*., 2008a].

The Northern San Francisco Bay Area is sliced by three major right-lateral strike-slip faults, the northern SAF, the Rodgers Creek fault and the Green Valley fault. The Rodgers Creek fault represents the North Bay continuation of the Hayward fault zone and the Green Valley fault is the northern extension of the Concord fault. North of the juncture with the San Gregorio fault, geodetic and geologic data suggest a SAF slip rate of 20-25 mm yr^{-1} [d'Alessio *et al*., 2005; Funning *et al*., 2007]. The remainder of the 40 mm yr^{-1} of Pacific plate to Sierra Nevada Great Valley microplate motion is primarily accommodated by the Rodgers Creek and the Green Valley faults. Both the Rodgers Creek fault [Funning *et al*., 2007] and the Green Valley fault (http://pubs.usgs.gov/of/2007/1367) accommodate some of their shallow slip budget by aseismic creep.

Near Point Reyes, the SAF separates two different geologic terranes. On the east side of the fault is the Franciscan Complex, made of a mixture of Mesozoic oceanic crustal rocks and sediments, which were accreted onto the North American continent during subduction of the Farallon plate. On the west side of the SAF lies the Salinian terrane, which is composed of Cretaceous granitic and metamorphic rocks, overlain by Tertiary sedimentary rocks and Quaternary fluvial terraces. Prescott et al. [1986] and Lisowski et al. [1991] describe an asymmetric deformation pattern along a trilateration-measured surface velocity profile across the SAF at Point Reyes, which can be explained by higher rigidities to the SW of the fault. Le Pichon et al. Le [2005], describe an asymmetric pattern further north along the SAF at Point Arena, but do not find significant asymmetry in the GPS data set of Savage et al. [Savage *et al*., 2004] at Point Reyes. [Chen and Freymueller, 2002], rely on near-fault strain rates determined from trilateration and GPS measurements to infer a 2-km-wide near-fault compliant zone with 50 % reduced rigidity near Bodega Bay and Tomales Bay. We use densely spaced GPS velocities and permanent scatterer InSAR data across the SAF to model the interseismic elastic loading in this area and evaluate changes in elastic properties across and within the fault zone. In 2007 we collected new GPS data at sites in Bodega Bay and Tomales Bay (Figure 6) that were last observed in 1996-2000 GPS measurements by Chen and Freymueller [2002].

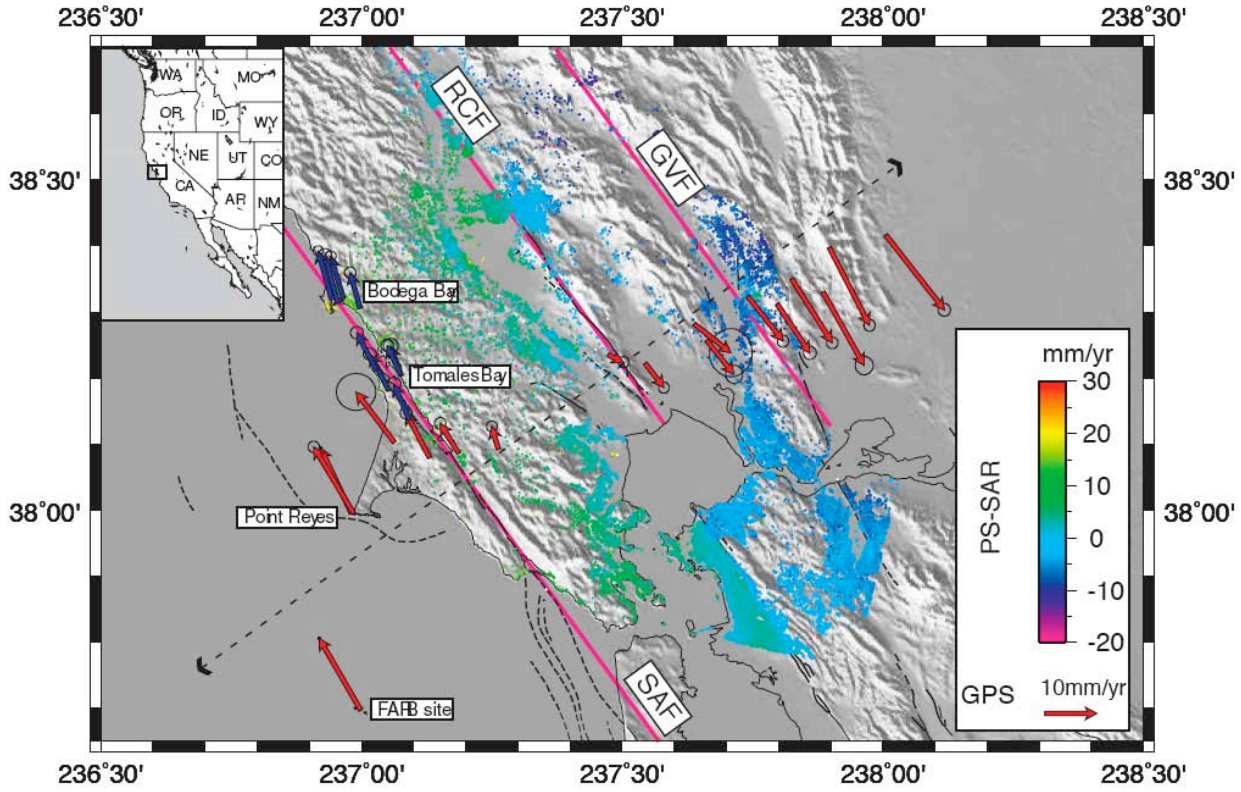

Figure 6. Map and SRTM topography of the northern Bay Area. The blue arrows are the data calulated from the 1996, 2000 (Chen and Freymueller [2002]) and 2007 (this study) campaign. The red arrows are the data from the BAVU 2 compilation. The colored dots are the along SAF strike projected velocities derived from PS-InSAR data from Funning et al. [2007]. The black dashed arrow represent the studied Point Reyes profile. The fault are in black continuous line while the modelled faults are in purple.

We first develop a simple 2D half-space dislocation model, based on three parallel faults (SAF, RCF and GVF) The best-fit model has a 23±1 mm yr^{-1} slip rate on the SAF, with a 14±2 km locking depth for a Chi^2=4.33. We find a 8±1 mm yr^{-1} slip rate on the RCF and 9±1 mm yr^{-1} on the GVF below locking depths of 5 ± 3 km and 4 ± 1 km, respectively, thus the whole system is accommodating 40 ± 3 mm yr^{-1} of fault parallel displacement (Figure 7). The measured velocity for the Farallon Island station is 4 to 5 mm yr^{-1} slower than the half-space model velocity and inconsistent with the observation that the velocity of the Farallon Island cGPS station with respect to the Pacific plate interior is only about 3 ± 1 mm yr^{-1} towards the southeast.

We next consider asymmetric models with a rigidity contrast across the SAF [Le Pichon *et al.*, 2005]. We continue to use the classic half-space dislocation model for the RCF and the GVF. We find that the modeled velocity profile better matches the data and especially the Farallon Island velocity with a 0.41 K ratio across the SAF. The corresponding Chi^2 is 2.63. This model suggest an 18±1 mm yr^{-1} slip rate on the SAF with a 10±2 km locking depth, a 11 mm yr^{-1} slip rate on the RCF with a 10 km locking depth and a 9 mm yr^{-1} slip rate on the GVF with a 5 km

locking depth. Thus, we infer that the Salinian terrane has a rigidity 1.4 times higher than the Franciscan complex to the east of the SAF. This conclusion is consistent with the type of terrane involved. The rigidity of the Salinian granite should be higher than the Franciscan oceanic mixture's one [Thurber *et al*., 2007].

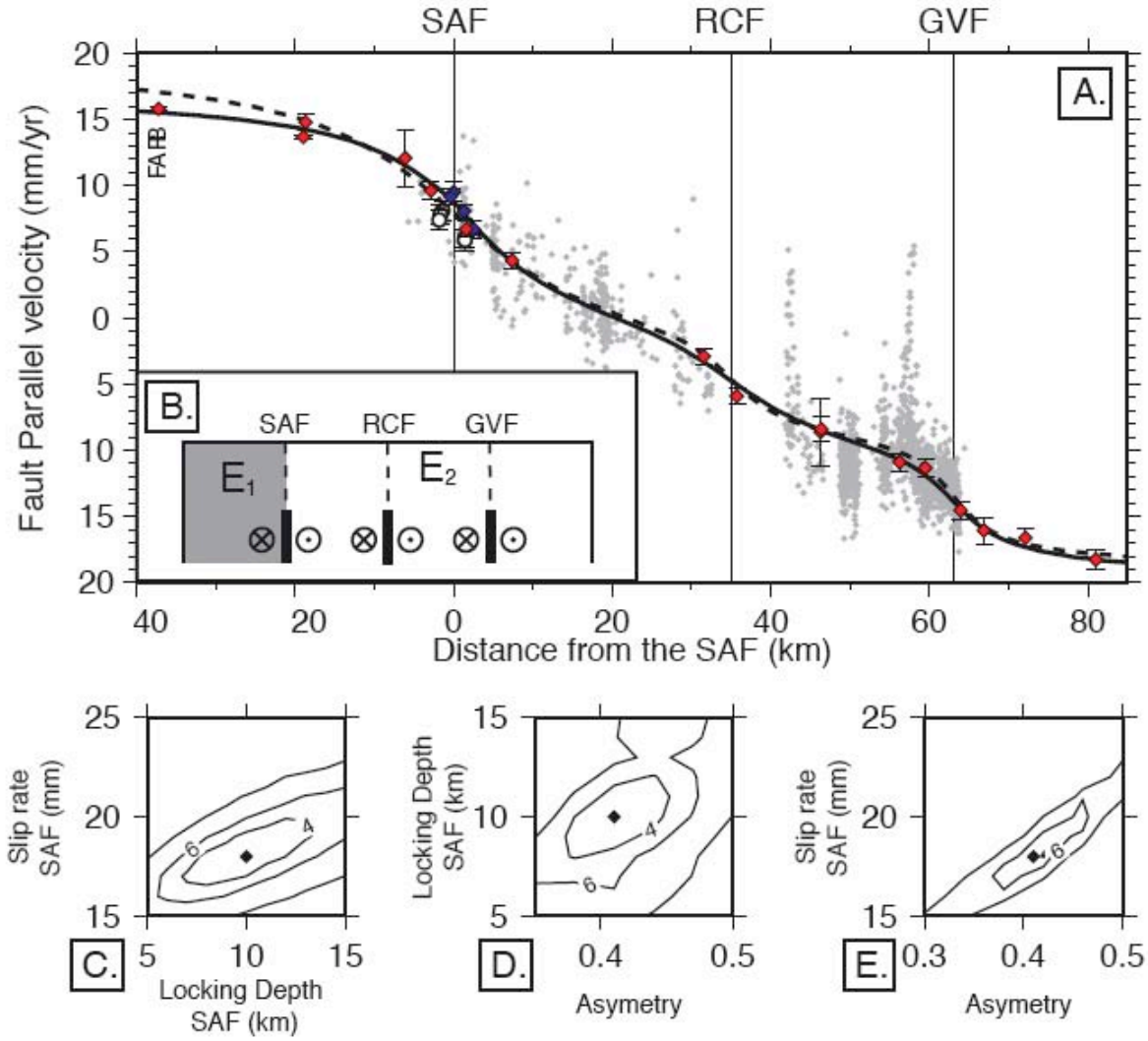

Figure 6. A. Best-fit dislocation models for the Point Reyes profile. The red dots are the fault-parallel projected GPS velocities from the BAVU 2 compilation with their associated error bars. The white dots are the fault-parallel projected GPS velocities from this study in Tomales Bay with their associated error bars, the blue dots correspond to the site velocities in Bodega Bay. The GPS velocities are calculated with respect to station LUTZ (121.865°W, 37.287°N). The grey dots are the PS-InSAR data (from Funning et al. [2007]). The dashed line is the best classic (elastic half-space) dislocation model. The continuous line is our preferred asymmetric model with a K ratio of 0.41 that better matches the observed velocity of the westernmost GPS site on the Farallon Islands. B. Geometry of the best fit dislocation model. The grey shaded zone corresponds to the high-rigidity block. C. Trade off between the locking depth and the slip rate on the SAF. Contoured values are the Chi^2 values. D. Trade off between the asymmetry ratio and the locking depth on the SAF. E. Trade off between the asymmetry ratio and the slip rate on the SAF.

There is a significant trade-off between the inferred slip rate on the SAF and the rigidity contrast across the fault, with smaller rigidity contrasts leading to higher inferred slip rates and deeper locking depth (Figure 7C-E). If the inferred slip rate is increased a little, the rigidity contrasts in the model needs to be lower and the locking depth deeper to produce the Farallon Island velocity.

The two networks across the SAF located further north, one in Tomales Bay and one in Bodega Bay, allow us to consider if the SAF represents a low-rigidity fault zone. In Bodega Bay, our preferred model is based on a deep compliant fault zone model, with the previously determined 18 mm yr^{-1} slip rate on the SAF, with a 15 km locking depth. The compliant zone is 50 % weaker than the surrounding medium and 2-km wide. But a classic homogeneous model with a 20 mm yr^{-1} slip rate and a 7 km locking depth on the SAF satisfies the near-field data as well, as predicted by the first-order trade-off between locking depth and the compliant fault zone rigidity contrast described in the previous section. Unfortunately, there are very few earthquakes from Point Reyes, up to Bodega Bay, so we cannot independently infer the local seismic-aseismic transition depth. However, in nearby areas to the south and east the depth above which 90 % of earthquakes occur is around 10 – 15 km and heat flow measurements in the area suggest similar locking depths [d'Alessio *et al*., 2005]. Thus, we prefer a 15 km locking depth and favor the low-rigidity CFZM model as the explanation for the localized deformation we observe.

4. DATA AVAILABILITY

Raw and RINEX formatted GPS data files for static surveys of markers in the San Francisco Bay area from 1994-2004. These files typically include greater than six continuous hours of data, recorded at a 30 s collection rate with a 10-degree elevation mask. Data from GPS campaigns are publicly available from the UNAVCO Campaign Data Holdings Archive. Both raw GPS data and accompanying metadata are included and freely accessible at http://facility.unavco.org/data/gnss/campaign.php. Data collected by our group for this project are archived under the PI Name (Burgmann) for campaigns named "Calaveras Fault", "Hayward Fault", "Central San Andreas" and "Loma Prieta."

Please see http://www.unavco.ucar.edu/data_support/data/general.html for policies regarding the use of these freely available data. Additional data used in this study included RINEX format files obtained from the U.S. Geological Survey and the Bay Area Regional Deformation Network (BARD). These files include campaign-style surveying (USGS) and continuous GPS stations (BARD) and are available at the NCEDC at UC Berkeley.

Processed GPS solutions, including the BAVU velocity field, time series and GAMIT-format solution files (h-files) are available via the BAVU web pages at:

http://seismo.berkeley.edu/~burgmann/RESEARCH/BAVU/

http://seismo.berkeley.edu/~houlie/bavu2_website/

http://seismo.berkeley.edu/~burgmann/RESEARCH/BAVU/FILES/gamit.html

Please cite:
d'Alessio, M. A., Johanson, I. A., Bürgmann, R., Schmidt, D. A., and M. H. Murray. 2005. Slicing up the San Francisco Bay Area: Block kinematics and fault slip rates from GPS-derived surface velocities. Journal of Geophysical Research, doi: 10.1029/2004JB003496.

GPS Processing

- station.info
- A Priori coordinate file

Results

- Daily h-files
- Monthly h-files
- Final Velocity h-file
- Final Velocities in ITRF2000NNR Reference Frame (Tab deliminated text)
- Final Velocities in North American Reference Frame (Tab deliminated text)

For more information regarding data availability, contact:

Dr. Roland Bürgmann
Department of Earth and Planetary Science, University of California, Berkeley
307 McCone Hall, Berkeley, CA 994720-4767
e-mail:burgmann@seismo.berkeley.edu

5. REFERENCES

Altamimi, Z., P. Sillard, and C. Boucher (2002), ITRF2000: A new release of the International Terrestrial Reference Frame for earth science applications, *Journal of Geophysical Research*, *107*, doi:10.1029/2001JB000561.

Arnadottir, T., and P. Segall (1994), The 1989 Loma Prieta earthquake imaged from inversion of geodetic data, *Journal of Geophysical Research*, *99*, 21,835-821,855.

Bürgmann, R., G. Hilley, A. Ferretti, and F. Novali (2006), Resolving vertical tectonics in the San Francisco Bay area from GPS and Permanent Scatterer InSAR analysis, *Geology*, *34*, 221-224.

Bürgmann, R., P. A. Rosen, and E. J. Fielding (2000), Synthetic aperture radar interferometry to measure Earth's surface topography and its deformation, *Annual Reviews of Earth and Planetary Sciences*, *28*, 169-209.

Bürgmann, R., P. Segall, M. Lisowski, and J. Svarc (1997), Postseismic strain following the 1989 Loma Prieta earthquake from GPS and leveling measurements, *Journal of Geophysical Research*, *102*, 4933-4955.

Chen, Q., and J. T. Freymueller (2002), Geodetic evidence for a near-fault compliant zone along the San Andreas fault in the San Francisco Bay Area, *Bull. Seism. Soc. Am.*, *92*, 656-671.

d'Alessio, M. A., I. A. Johansen, R. Bürgmann, D. A. Schmidt, and M. H. Murray (2005), Slicing up the San Francisco Bay Area: Block kinematics and fault slip rates from GPS-derived surface velocities, *Journal of Geophysical Research*, *110*, doi:10.1029/2004JB003496.

Funning, G., R. Bürgmann, A. Ferretti, F. Novali, and A. Fumagalli (2007), Creep on the Rodgers Creek fault from PS-InSAR measurements, *Geophys. Res. Lett.*, *34*, doi:10.1029/2007GL030836.

Herring, T. A. (2005), GLOBK, Global Kalman filter VLBI and GPS analysis program, Version 10.2, *Mass. Instit. of Tech., Release 10.2*.

Hilley, G. E., R. Bürgmann, A. Ferretti, F. Novali, and F. Rocca (2004), Dynamics of slow-moving landslides from permanent scatterer analysis, *Science*, *304*, 1952-1955.

Jolivet, L., R. Bürgmann, and N. Houlié (2008a), GPS exploration of the elastic properties across and within the Northern San Andreas Fault zone and heterogeneous elastic dislocation models, *Geophys. Res. Lett., in preparation*.

Jolivet, R., R. Cattin, N. Chamot-Rooke, C. Lasserre, and G. Peltzer (2008b), Thin-plate modelling of interseismic deformation and asymmetry across the Altyn Tagh fault zone, *Geophys. Res. Lett.*, *35*, doi:10.1029/2007GL031511.

Kenner, S. J., and P. Segall (2003), Lower crustal structure in northern California: Implications from strain-rate variations following the 1906 San Francisco earthquake, *Journal of Geophysical Research*, *108*, doi: 10.1029/2001JB000189.

King, R. W., and Y. Bock (2005), Documentation for the GAMIT GPS Analysis software, *Mass. Instit. of Tech., Scripps Inst. Oceanogr., Release 10.2*.

Knudsen, K. L., J. M. Sowers, R. C. Witter, C. M. Wentworth, and E. J. Helley (2000), Map of Quaternary deposits and liquefaction susceptibility, nine-county San Francisco Bay region, California, *U.S. Geol. Surv. Open File Rep.*, *00-444*, http://pubs.usgs.gov/of/2000/of2000-2444/.

Le Pichon, X., C. Kreemer, and N. Chamot-Rooke (2005), Asymmetry in elastic properties and the evolution of large continental strike-slip faults, *J .Geophys. Res.*, *110*, doi:10.1029/2004JB003343.

Lisowski, M., J. C. Savage, and W. H. Prescott (1991), The velocity field along the San Andreas fault in central and southern California, *Journal of Geophysical Research*, *96*, 8369-8389.

Marshall, G. A., R. S. Stein, and W. Thatcher (1991), Faulting geometry and slip from co-seismic elevation changes: The October 17, 1989 Loma Prieta, California, earthquake, *Bull. Seism. Soc. Am.*, *81*, 1660-1693.

Okada, Y. (1985), Surface deformation due to shear and tensile faults in a half-space, *Bull. Seism. Soc. Am.*, *75*, 1135-1154.

Parsons, T. (2002), Post-1906 stress recovery of the San Andreas fault system calculated from three-dimensional finite element analysis, *Journal of Geophysical Research*, *107*, 10.1029/2001JB001051.

Pollitz, F., W. H. Bakun, and M. Nyst (2005), A physical model for strain accumulation in the San Francisco Bay region: Stress evolution since 1838 *Journal of Geophysical Research*, *109*, doi:10.1029/2004JB003003.

Pollitz, F., R. Bürgmann, and B. Romanowicz (1997), Postseismic stress diffusion: transient velocity of oceanic lithosphere, *EOS, Transactions American Geophysical Union*, *78*, 155.

Pollitz, F., R. Bürgmann, and P. Segall (1998), Joint estimation of afterslip rate and postseismic relaxation following the 1989 Loma Prieta earthquake, *Journal of Geophysical Research*, *103*, 26,975-926,992.

Prescott, W. H., and S.-B. Yu (1986), Geodetic measurement of horizontal deformation in the northern San Francisco Bay region, California, *Journal of Geophysical Research*, *91*, 7475-7484.

Savage, J. C., and R. O. Burford (1973), Geodetic determination of relative plate motion in central California, *Journal of Geophysical Research*, *78*, 832-845.

Savage, J. C., W. Gan, W. H. Prescott, and J. L. Svarc (2004), Strain accumulation across the Coast Ranges at the latitude of San Francisco, 1994–2000, *Journal of Geophysical Research*, *109*, doi: 10.1029/2003JB002612.

Savage, J. C., M. Lisowski, and J. L. Svarc (1994), Postseismic deformation following the 1989 (M = 7.1) Loma Prieta, California, earthquake, *Journal of Geophysical Research*, *99*, 13757-13765.

Schmalzle, G., T. Dixon, R. Malservisi, and R. Govers (2006), Strain accumulation across the Carrizo segment of the San Andreas Fault, California: Impact of laterally varying crustal properties, *Journal of Geophysical Research*, *111*, doi:10.1029/2005JB003843.

Schmidt, D. A., and R. Bürgmann (2003), Time dependent land uplift and subsidence in the Santa Clara valley, California, from a large InSAR data set, *Journal of Geophysical Research*, *108*, doi:10.1029/2002JB002267.

Schmidt, D. A., R. Bürgmann, R. M. Nadeau, and M. A. d'Alessio (2005), Distribution of aseismic slip-rate on the Hayward fault inferred from seismic and geodetic data, *Journal of Geophysical Research*, *110*, doi:10.1029/2004JB003397.

Segall, P., R. Bürgmann, and M. Matthews (2000), Time dependent deformation following the 1989 Loma Prieta earthquake, *Journal of Geophysical Research*, *105*, 5615-5634.

Thatcher, W. (1983), Nonlinear strain buildup and the earthquake cycle on the San Andreas fault, *Journal of Geophysical Research*, *88*, 5893-5902.

Thurber, C., H. Zhang, F. Waldhauser, J. Hardebeck, A. J. Michael, and D. Eberhart-Phillips (2007), Three-Dimensional Compressional Wavespeed Model, Earthquake relocations, and Focal Mechanisms for the Parkfield, California, *Bull. Seism. Soc. Am.*, *96*, S38-S49.